Published in final edited form as:
Neuroimage. 2013 November 1; 81: 213–221. doi:10.1016/j.neuroimage.2013.05.016.

Distributed effects of methylphenidate on the network structure of the resting brain: a connectomic pattern classification analysis

Chandra Sekhar Sripada[1,§,*], **Daniel Kessler**[1,§], **Robert Welsh**[1,2], **Michael Angstadt**[1], **Israel Liberzon**[1,3], **K. Luan Phan**[4], and **Clayton Scott**[5,6]

[1]Department of Psychiatry, University of Michigan, Ann Arbor, MI

[2]Department of Radiology, University of Michigan, Ann Arbor, MI

[3]Mental Health Service, VA Ann Arbor Healthcare System, Ann Arbor, MI

[4]Department of Psychiatry, University of Illinois at Chicago

[5]Department of Electrical Engineering and Computer Science, University of Michigan, Ann Arbor, MI

[6]Department of Statistics, University of Michigan, Ann Arbor, MI

Abstract

Methylphenidate is a psychostimulant medication that produces improvements in functions associated with multiple neurocognitive systems. To investigate the potentially distributed effects of methylphenidate on the brain's intrinsic network architecture, we coupled resting state imaging with multivariate pattern classification. In a within-subject, double-blind, placebo-controlled, randomized, counterbalanced, cross-over design, 32 healthy human volunteers received either methylphenidate or placebo prior to two fMRI resting state scans separated by approximately one week. Resting state connectomes were generated by placing regions of interest at regular intervals throughout the brain, and these connectomes were submitted for support vector machine analysis. We found that methylphenidate produces a distributed, reliably detected, multivariate neural signature. Methylphenidate effects were evident across multiple resting state networks, especially visual, somatomotor, and default networks. Methylphenidate reduced coupling within visual and somatomotor networks. In addition, default network exhibited decoupling with several task positive networks, consistent with methylphenidate modulation of the competitive relationship between these networks. These results suggest that connectivity changes within and between large-scale networks is potentially involved in the mechanisms by which methylphenidate improves attention functioning.

[*]**Corresponding Author:** Chandra Sekhar Sripada, MD, PhD, Department of Psychiatry, University of Michigan, Rachel Upjohn Building, Room 2743, 4250 Plymouth Road, Ann Arbor, MI 48109-2700, sripada@umich.edu, Phone: (734) 936-9527, Fax: (734) 936-7868.
[§]These authors contributed equally

Conflicts of Interest: The authors declare no conflict of interest.

Keywords

methylphenidate; fMRI; resting state; multivariate pattern classification; connectome; intrinsic connectivity networks

Methylphenidate (MPD) is a psychostimulant medication that is a highly efficacious and widely prescribed treatment for attention deficit hyperactive disorder (ADHD). MPD produces improvements in attention, motoric control, executive processing, and memory (Swanson et al., 2011)—cognitive functions associated with distributed neurocognitive systems. Previous studies have emphasized MPD effects on specific brain regions during tasks specifically tailored to elicit selective activation (Cortese et al., 2012). More global patterns of MPD effects on connectivity across distributed brain networks are still poorly understood.

Intrinsic connectivity networks (ICNs) consist of distributed brain regions exhibiting coherent activity (Greicius et al., 2003), and which are reliably detected (Damoiseaux et al., 2006) from low-frequency oscillations of the blood oxygenation level dependent (BOLD) signal during the resting state. Convergent evidence indicates that ICNs constitute fundamental organizational elements of human neural architecture (Beckmann et al., 2005; Laird et al., 2011). Individual ICNs have been implicated in specific neurocognitive functions such as attention control and somatomotor processing (Menon and Uddin, 2010; Yeo et al., 2011). Moreover, aberrant connectivity within specific ICNs is linked to clinically-relevant symptom dimensions across psychiatric disorders (Menon, 2011). Thus investigating alterations in ICNs during the resting state constitutes a powerful method to understand distributed effects of acute drug administration.

A number of specific ICNs may be targets of MPD effects. The default mode network (DMN) is a network of midline and lateral parietal regions that is implicated in internally directed mentation (Raichle et al., 2001) and lapses of attention (Weissman et al., 2006), and it exhibits a competitive relationship with task-positive networks (Corbetta and Shulman, 2002), such as dorsal and ventral attention networks and frontoparietal control network. Previous task-based fMRI studies (Liddle et al., 2011; Nagano-Saito et al., 2008; Peterson et al., 2009; Tomasi et al., 2011) have suggested the competitive relationship between these networks (Fox et al., 2005) is enhanced by dopamine. Thus we hypothesized that MPD would produce greater segregation between DMN and task-positive networks during the resting state. We also had a priori hypotheses about MPD effects on motor processing networks and visual network. Existing circuit models propose dopamine-mediated interactions between striatum and motor cortex (Alexander et al., 1986) as well as striatum and cerebellum (Hoshi et al., 2005), and previous fMRI studies with acute administration of dopamine modulators [L-dihydroxyphenylalanine (L-Dopa), cocaine] found altered connectivity in multiple motor regions including striatum, cerebellum, and motor cortex (Cole et al., 2012; Kelly et al., 2009; Li et al., 2000). Additionally, Li and colleagues (2000) found that cocaine reduced connectivity within visual cortex, with evidence suggesting that greater decoherence in visual cortex is associated with high attention states (McAvoy et al., 2012; Nauhaus et al., 2009). Thus we predicted that MPD would modulate resting state connectivity in motor regions including striatum, somatomomotor network, and cerebellum, and would reduce connectivity within visual network.

Seed-based methods are commonly used to investigate functional connectivity. These methods have the advantage of identifying connectivity changes at well-defined regions, but are they also restricted to investigating a single, or a handful, of selected regions, and require potentially arbitrary choices of which a priori regions to investigate. In this study we

coupled two methods that help to overcome restrictions with standard seed-based methods. We used connectomic imaging methods to identity functional connectivity pairwise between 1080 regions of interest (ROIs) placed at regular intervals throughout the brain. Additionally, we used multivariate pattern classification, which allows connectivity across multiple regions and networks to simultaneously inform classification decisions (Heinzle et al., 2012).

Methods and Materials

Participants and pharmaco-fMRI design

In this within-subject, double-blind, placebo-controlled, randomized, counterbalanced, cross-over study, 32 right-handed healthy volunteers (16 females; age 20.6 +/− 2.0 years, range 18–27) participated in two fMRI scanning sessions separated by approximately 1 week. Participants received either 40mg MPD or PBO 60 minutes prior to resting state scanning. The dose of MPD was higher than typically used in clinical practice in order to enhance blood levels, and predicted psychological and neural effects, in an acute dosing context, consistent with recent studies (Clatworthy et al., 2009; Schlosser et al., 2009b).

All participants completed a Visual Analogue Scale (VAS) immediately prior to drug ingestion as well as 30, 60, and 140 minutes afterwards (Figure 1). This scale consists of 20 items that measure cognitive and emotional state using adjective descriptors (e.g., ‘stimulated’, ‘drowsy’), and responses were recorded on 4-inch bars anchored with ‘Not At All’ and ‘Extremely’. Post-ingestion measures were adjusted by subtracting baseline responses immediately prior to drug ingestion. They were then compared between PBO versus MPD sessions via repeated measures ANOVA.

Resting State Paradigm

During resting state scans, a black fixation cross on a white background was displayed in the center of the screen for 6 minutes. Participants were instructed to relax and keep their eyes open and fixed on the cross. Participants next completed an attention control task and a decision-making task, which are described in a separate report. Heart rate and respiration measurements were acquired for group comparisons using paired *t*-tests.

Magnetic Resonance Imaging Image Acquisition

MRI scanning occurred on a Philips 3.0 Tesla Achieva X-series MRI (Best, The Netherlands). We obtained a medium resolution T1-weighted anatomical scan, 180 functional volumes with a T2*-weighted, echoplanar acquisition sequence [GRE; repetition time, 2000 ms; echo time, 25ms; flip angle, 90°; field of view, 22cm; 42 slice; thickness/skip, 3.0/0mm matrix size equivalent to 64×64], and a high-resolution T1-weighted scan for anatomic normalization [26cm FOV; thickness/skip, 1.0/0mm].

Preprocessing

A standard series of processing steps was performed using statistical parametric mapping (SPM8; www.fil.ion.ucl.ac.uk/spm). Scans were reconstructed, slicetime corrected (sequential ascending), and realigned to the first scan in the experiment to correct for head motion, and co-registered with the high-resolution T1-weighted image (the medium-resolution T1-weighted image was co-registered with the functional scans as an intermediate step and then the high-resolution T1-weighted image was coregistered with the medium-resolution T1-weighted image). Normalization was performed using the voxel-based morphometry toolbox implemented in SPM8. The high-resolution T1-weighted image was segmented into tissue types, bias-corrected, registered to MNI space, and then normalized using Diffeomorphic Anatomical Registration Through Exponentiated Lie Algebra

(DARTEL) (Ashburner, 2007). Smoothing of functional data was performed with an $8mm^3$ kernel. Motion parameters were checked in order to identify and exclude all scans with greater than 2mm movement. Summary motion statistics were calculated (mean displacement, mean angle) and were compared across drug conditions via paired samples Wilcoxon signed rank tests to account for non-normally distributed data.

In order to produce a whole-brain resting state functional connectome, we placed 4.25mm radius ROIs encompassing 19 3x3x3mm voxels in a regular grid spaced at 12mm intervals throughout the brain, yielding 1080 ROIs in total. Spatially averaged time series were extracted from each of these ROIs. White matter and cerebrospinal fluid masks were generated from the VBM-based tissue segmentation step noted above, and eroded using FSL-Erode to eliminate border regions of potentially ambiguous tissue-type. Next, regression was performed to remove the effects of nuisance variables, including six motion regressors generated from the realignment step, as well as their first derivatives, and the top five principal components of the BOLD time series extracted from each of the white matter and cerebrospinal fluid masks—a method that has been demonstrated to also effectively remove signals arising from the cardiac and respiratory cycle (Glover et al., 2000). The time-series for each ROI was band-passed filtered in the .01 – .10 Hz range, and Pearson product-moment correlation coefficients were then calculated pairwise between time courses for each of the 1080 ROIs, yielding 582,120 total features. A Fisher's r-z transform was applied to improve distributional properties of the correlation values.

Multivariate pattern classification

Feature pruning

We utilized univariate feature pruning (Guyon and Elisseeff, 2003) to remove features unrelated to classification and to accelerate computation, consistent with recent fMRI pattern classification studies (Mwangi et al., 2012; Zeng et al., 2012). For each feature, a paired sample *t*-value was calculated for the MPD versus PBO maps. Features were ranked by the magnitude of *t*-value (unsigned) and the top *n* features in this ranking were retained for classification. Based on pilot testing of other pharmaco-fMRI datasets (Sripada and Phan, personal communication), pruned feature sets of sizes {50, 100, 500, 1000, 5000, 10000, ALL} were initially tested, with additional values to be tested if relatively clear accuracy peaks failed to be identified.

Classification and performance evaluation

We used support vector machine (SVM) (Cortes and Vapnik, 1995) implemented in SVM^{light} (Thorsten Joachims, http://svmlight.joachims.org/). We used softmargin SVM that allows some misclassifications in order to obtain a wider classification margin (the C parameter was set to the SVM^{light} default: [avg $\mathbf{x}^*\mathbf{x}$] ^-1, where $\mathbf{x}$ is the feature vector), and a linear kernel. Classifier accuracy was assessed with leave-one-out cross-validation (LOOCV). Feature pruning was performed within each fold of the LOOCV to avoid bias. Classifier performance was compared with a binomial distribution $B(p,n)$, with p=0.5 and n=32 samples (Bishop, 2007; Heinzle et al., 2012). Because a slightly different set of features was retained during feature pruning at each fold of the LOOCV, we identified the 'consensus connectome', i.e., the subset of features that were retained at every fold of the LOOCV (Dosenbach et al., 2010; Zeng et al., 2012), as the basis for visualization and interpretation.

Visualization

Nodes in the consensus connectome were labeled according their network affiliation. We utilized the network parcellation of Yeo and colleagues (Yeo et al., 2011) who investigated

resting state networks in 1000 healthy individuals. Their parcellation has the advantage of being derived from grid-based connectomic methods applied to resting state scans, highly similar to the current study. Given strong a priori hypotheses about MPD effects on striatal connectivity (Kelly et al., 2009), the Yeo parcellation map was augmented with an additional striatal mask, created using the AAL system (Tzourio-Mazoyer et al., 2002), in order to label any nodes that fell within this region.

Paired SVM

In this within-subject pharmaco-fMRI study, each subject underwent two scanning sessions and produced two connectivity maps, one from their PBO session and one from their MPD session. In order to account for the within-subject nature of the data, we utilized a 'paired SVM' approach that uses delta maps produced by subtracting each subject's drug and placebo maps against each other as the basis for classification. Though the paired SVM idea (Scholkopf et al., 2001) and related approaches (Connolly and Liang, 1988) have been discussed and formalized in the literature, they are not widely used by researchers, and thus we expand on the rationale for this approach below.

Within-subject designs are often used in order to provide information about the *differential* contribution of the intervention condition on neural activation, over and above some baseline. That is, it is assumed subjects vary in neural activation at baseline, and the goal is to discern whether the intervention differentially affects the brain, factoring out this baseline variation. In univariate parametric statistics, a paired *t*-test is used for this purpose. This test computes delta maps between the intervention condition and baseline, and performs statistical tests on these delta maps. Paired SVM offers an analogous approach in the SVM framework.

Suppose that MPD does in fact produce highly reliable changes in functional connectivity. For example, suppose that relative to PBO baseline, MPD reliably increases connectivity in edges $i_1 \ldots i_i$ and reliably decreases connectivity in edges $d_1 \ldots d_j$. But let us also suppose that each subject has a variable baseline, so that while the differential change induced by MPD relative to PBO baseline is highly reliable, the actual connectivity values observed during MPD at features $i_1 \ldots i_i$ and $d_1 \ldots d_j$ vary considerably across subjects. Given these suppositions, consider the unpaired versus paired approaches to SVM classification.

An unpaired SVM approach ignores the within-subject structure of the data. Each scan is labeled as 'PBO' or 'MPD' and the SVM classifier attempts to learn how to distinguish these two classes. The trained classifier is then applied to new test examples and attempts to predict whether they are from the class 'PBO' versus 'MPD'. The problem with this approach is most apparent when we consider certain kinds of test cases. Suppose a certain subject, S*, has unusually high baseline connectivity in features $i_1 \ldots i_i$ and/or unusually low connectivity in features $d_1 \ldots d_j$. Nonetheless, MPD exerts the same directional effect for this subject as it does for other subjects with more usual baseline values—that is, MPD increases connectivity in in features $i_1 \ldots i_i$ and decreases connectivity in features $d_1 \ldots d_j$. An unpaired SVM classifier will tend to predict that this subject's PBO scan is from the class 'MPD', owing to this subject's unusual baseline values in features $i_1 \ldots i_i$ and $d_1 \ldots d_j$. To prevent this result, and more generally to account for each subject's potentially variable baseline connectivity, we need some way to provide the classifier with richer information not simply about the value of features, but rather about the differences in values for features across PBO versus MPD conditions.

In a paired SVM approach, rather than contributing a PBO and MPD map, each subject instead contributes an MPD-PBO map and PBO-MPD map, and the classifier attempts to distinguish the 'MPD-PBO' class from the 'PBO-MPD' class. Note that each subject's

MPD-PBO example will differ from that subject's PBO-MPD example by reversal of sign on all the features. As a consequence, the optimal hyperplane will be unbiased, i.e., a hyperplane that goes through the origin. Despite this restriction on the placement of the optimal hyperplane, the paired SVM classification problem is still well posed and, importantly, it addresses the critical question of *differential effects* that was not possible to address in the unpaired framework. In order to learn the difference between MPD-PBO versus PBO-MPD delta maps and successfully generalize to new examples, the paired SVM classifier must learn which are the features at which MPD reliably exerts additional effects over and above PBO baseline. In particular, given our supposition that MPD reliably increases connectivity in edges $i_1 \ldots i_i$ and reliably decreases connectivity in edges $d_1 \ldots d_j$, then the weight vector of a trained paired SVM classifier will reflect the importance of features $i_1 \ldots i_i$ and $d_1 \ldots d_j$ in distinguishing MPD-PBO maps from PBO-MPD maps. Recall that cases like subject S* (who had unusually high baseline connectivity in features $i_1 \ldots i_i$ and/or unusually low baseline connectivity in features $d_1 \ldots d_j$) presented a problem for unpaired SVM. However, a paired SVM classifier that has been trained to distinguish MPD-PBO versus PBO-MPD maps will not have any special trouble with S*. By posing the classification problem in terms of delta maps, we have controlled for each subject's potentially variable baseline, and have forced the classifier to focus on the differential effects of MPD over and above PBO baseline. In short then, within-subject designs are often used to address questions about the effects of an intervention over and above baseline. A paired SVM represents an attractive way to address this type of question in an SVM framework.

In using paired SVM in the context of a leave-one-out cross-validation procedure, we performed the following steps. First, we calculated MPD-PBO and PBO-MPD delta maps for each of n subjects, yielding n*2 maps. Next, at each fold of the LOOCV procedure, we trained a two-class linear SVM classifier on the delta maps from all the subjects except the subject held out. That is, the classifier was presented with (n-1)*2 examples. This trained classifier was next used to assign class labels to the two examples from the held out subject, and mean accuracy across all folds of the LOOCV was computed.

In an online technical report (Scott, 2012; http://www.eecs.umich.edu/techreports/systems/cspl/cspl-412.pdf), we demonstrate that two-class linear SVM on delta maps is formally identical to a theoretically and empirically validated variant of SVM called one-class SVM. This is analogous to the fact that paired-sample t-tests are formally identical to one- sample t-tests performed on delta maps. The connection between our paired SVM approach and one-class SVM has an added advantage of suggesting how to extend the method to use of non-linear kernels, which could aid in detection of complex interactive effects among features in classification of within-subject data. Since one-class SVM is not as well known or as easily available to researchers, we continue to present our results in terms of two-class SVM on MPD-PBO and PBO-MPD delta maps. This way of presenting the analysis is simpler and more intuitive, and makes available to researchers a powerful way in the two-class SVM framework to classify paired maps that arise from within-subject designs.

Results

Participants' subjective reports of drug effects on the VAS scale were significantly different during the MPD session versus PBO sessions. There was a significant main effect of treatment, such that during the MPD session, participants were more 'stimulated' (p<0.039), 'energetic' (p<0.007), 'alert' (p<0.002), and 'focused' (p<0.026), and less 'tired' (p<0.013), and 'drowsy' (p<0.048). Of note, no treatment x time point interaction was observed. Participants' own guesses of whether they received MPD versus PBO did not deviate from

chance at any time point immediately prior to, and after (30, 60, 140 minutes) drug ingestion (binomial tests: all p's>0.59).

Motion and physiological data

There were no movements greater than 2 millimeters for any session. Participants' PBO and MPD sessions did not differ in mean spatial displacement or mean angle (Wilcoxon signed ranked tests: p's>0.68), or in heart rate or respiratory rate (paired t-tests: p's>0.70).

Pattern Classification Analysis

We found accuracy peaks at both 50 and 500 features (Figure 2). With 50 features in the pruned feature set, the classifier exhibited 81% accuracy (p = 0.001; binomial test) in classifying the delta maps (MPD-PBO and PBO-MPD) of each withheld subject, while with 500 features accuracy was 78% (p = 0.002; binomial test). Accuracy was comparable to that achieved in a recent fMRI pattern classification of MPD effects during a working memory task (Marquand et al., 2011). We report the results for both classifiers (i.e., 50 and 500 features). Of note, even though classification accuracy was slightly better at 50 features, performance at both feature set sizes is quite similar, and other things being more or less equal, a larger feature set should have better resolution in reflecting the way edges are distributed across networks (i.e., this pattern should be less susceptible to chance variation due to there being too small a sample of edges).

50 feature classifier—With 50 edges in the pruned feature set, there were 26 edges in the consensus connectome, i.e., the set of edges that contributed to classification across all folds of the LOOCV. Edges of the consensus connectome were concentrated in just a few major networks. In particular, 23 of the 26 edges involved three networks (that is, at least one node associated with these 23 edges was in these three networks): visual network (14 edges), somatomotor network (9 edges), and default network (6 edges). The visual network exhibited 10 intra-network connections. The default network decoupled with two task positive networks, ventral attention network (2 edges) and somatomotor network (1 edge). The cross-tabulation of edges with respect to the seven ICNs as well as striatum is shown in Table 1.

Baseline connectivity under PBO and change under MPD: The mean connectivity during PBO for edges in the consensus connectome was 0.29 (Pearson's r) and was greatest in edges that were entirely within the visual network (Figure 3). For the 10 edges that were entirely within the visual network, mean baseline connectivity was r=0.52, while the remaining edges exhibited baseline correlation of 0.10. Most edges decreased in strength in the MPD session compared to the PBO session (22 of 26 decreased; see Table 1, Figure 3). Mean changes in correlation were similar within visual network compared to outside visual network (within visual: delta r=0.14, delta z=0.17; outside visual: delta r=0.14, delta z=0.14).

500 feature classifier

Network affiliation of consensus edges: With 500 edges in the pruned feature set, there were 240 edges in the consensus connectome (Table 2). Similar to the 50 feature classifier, edges of the consensus connectome tended to be concentrated in just a few major networks. In particular, 228 of the 240 edges involved three networks (that is, at least one node associated with these 228 edges was in these three networks): default network (80 edges), somatomotor network (79 edges), and visual network (69 edges). Three task positive networks were also well represented in the consensus connectome: dorsal attention network (28 edges), ventral attention network (34 edges), and frontoparietal network (23 edges). The

visual network and somatomotor network exhibited a substantial number of intra-network connections. In both networks, there were 27 edges within the network that decreased in strength (Figure 4a and 4c). The default network exhibited decoupling with major task-positive networks (Figure 4e) including somatomotor network (13 edges) and ventral and dorsal attention networks (10 edges). It also decoupled with limbic network (10 edges), especially with medial and lateral orbitofrontal regions.

Baseline connectivity under PBO and change under MPD: Similar to the 50 edge classifier, mean connectivity during PBO was greatest in edges that were entirely within the visual network (r=0.59). Excluding visual network, mean baseline connectivity in the consensus connectome was weaker, but still modestly positive (r=0.12). Again, similar to the 50 feature classifier, a substantial majority of the edges in consensus connectome decreased in strength in the MPD session compared to the PBO session (172 of 240 decreased; see Table 2, Figure 4). The 68 edges that increased in strength primarily linked pairs of regions that were in networks associated with attention and motor control, including the ventral attention network, somatomotor network, and striatum. Mean changes in correlation were similar within visual network compared to outside visual network (within visual: delta r =0.11, delta z=0.16; outside visual: delta r=0.14, delta z=0.14).

Discussion

We investigated the distributed effects of MPD on the network structure of the resting brain using connectomic imaging coupled with multivariate pattern classification. We demonstrate that MPD produces a reliable multivariate neural signature. MPD's effects were evident across several ICNs, including visual, somatomotor, and default networks. Methylphenidate reduced coupling within visual and somatomotor networks. In addition, default network exhibited decoupling with several task positive networks, consistent with methylphenidate modulation of the competitive relationship between these networks. These results suggest that connectivity changes within and between large-scale networks is potentially involved in the mechanisms by which methylphenidate improves attention functioning. Moreover, this study goes beyond existing seed-based connectivity methods and demonstrates that connectomic imaging coupled with multivariate pattern classification can delineate the distributed effects of acute drug administration on large-scale brain networks.

We found that MPD produced widespread changes in patterns of connectivity across distributed resting state brain networks. These diffuse alterations are consistent with known cellular and systems level effects of the drug. MPDs mechanism of action involves blockade of dopamine and norepinephrine re-uptake transporters (Volkow et al., 2002). Positron emission tomography (PET) shows that MPD significantly increases levels of extracellular dopamine in striatum (Schiffer et al., 2006; Volkow et al., 2002; Volkow et al., 1998), as well as prefrontal and thalamic brain regions (Montgomery et al., 2007), while it increases norepinephrine availability in thalamus, locus coeruleus, and to a lesser extent, medial and lateral PFC (Hannestad et al., 2010). These neurotransmitters are in turn implicated in fundamental regulatory functions that impact distributed circuits, including attention networks (Arnsten and Li, 2005; Nieoullon, 2002; Posner and Rothbart, 2007; Ramos and Arnsten, 2007), motor processing regions (Brooks, 2001), and mesolimbic circuits involved in motivation and reward (McClure et al., 2003; Robbins, 2005). Previous fMRI studies have examined MPD effects primarily in the context of cognitively demanding tasks (Liddle et al., 2011; Marquand et al., 2011; Mehta et al., 2004; Peterson et al., 2009; Rubia et al., 2009). The present study extends these results by providing clear evidence that during the resting state, even in the absence of cognitive task performance, MPD produces a distributed, reliably detected multivariate neural signature.

With both the 50 and 500 feature classifiers, the consensus connectomes included multiple edges within visual network that deceased in connectivity under MPD (Figure 3a). This result is consistent with a previous resting state fMRI study by Li and colleagues (Li et al., 2000) who used a seed-based approach and found reduced connectivity within visual cortex due to cocaine, a potent releaser of synaptic dopamine. One interpretation of this finding is in terms growing evidence that links diminished neuronal coherence within visual cortex, especially between homotopic regions, with enhanced attentional states—for example eyes open versus eyes closed rest (McAvoy et al., 2012) and strong visual stimulation (Nauhaus et al., 2009). This hypothesis is further supported by a pharmaco-fMRI study (Ricciardi et al., 2012) that found physostigmine, an acetecholinesterase inhibitor that increases alertness and attention, reduces connectivity within the visual network during attention processing. Thus it is possible that our finding of decreased in connectivity within the visual network during MPD sessions reflects a high attention state produced by the drug.

With both the 50 and 500 feature classifiers, we observed prominent effects of MPD on the resting state connectome involving the somatomotor network (Figure 3, Figure 4c, Figure 4d), and striatal regions (Table 1 and Table 2). These results are consistent with existing circuit models that propose dopamine-mediated interactions between striatum and motor cortex (Alexander et al., 1986) as well as striatum and cerebellum (Hoshi et al., 2005). Previous fMRI studies have found that dopamine modulators including MPD and L-dopa enhance activation in motor regions including striatum, primary and secondary motor cortex, and cerebellum (Muller et al., 2005; Schlosser et al., 2009a), and normalize the activation deficits in these regions observed in patient populations such as ADHD and Parkinson's (Buhmann et al., 2003; Haslinger et al., 2001; Rubia et al., 2009). Our findings thus add to recent evidence involving other dopamine modulators [e.g., L-dopa (Cole et al., 2012; Kelly et al., 2009); haloperidol (Cole et al., 2012; Tost et al., 2010)], in suggesting that dopaminergic modulation of motor processing regions observed during task are also evident during the resting state.

We found in evidence from the 500 feature classifier that multiple regions of default network reduced their coupling with task positive ICNs including ventral attention network, dorsal attention network, and somatomotor network (Figure 4e). Default network regions also decoupled with medial and lateral orbitofrontal regions, which in previous studies have been associated with attention control (Hampshire and Owen, 2006) and emotion regulation (Ochsner and Gross, 2005). One interpretation of this finding is in terms of increased segregation between default network and task positive ICNs, which may also be related to the mechanism by which MPD produces enhanced attention functioning (Sonuga-Barke and Castellanos, 2007). During externally-oriented tasks, the DMN and task positive networks exhibit reciprocal interactions (McKiernan et al., 2003) with increased task-related activity related to suppression of DMN activity. DMN intrusion during tasks associated with lapses of attention (Weissman et al., 2006), and poorer task performance. suggesting that information processing in task-positive networks is optimized when default network intrusions are reduced. Moreover, dopaminergic modulation appears to alter the relationship between DMN and task positive ICNs. In particular, during attention tasks, methylphenidate administration increases activation of task positive regions and deactivation of DMN (Liddle et al., 2011; Peterson et al., 2009; Tomasi et al., 2011), while dopamine depletion reduces task-induced deactivations (Nagano-Saito et al., 2008). The reciprocal relationship between DMN and task-positive ICNs is also present during the resting state (Fox et al., 2005), and the degree of segregation between these two networks may be an important determinant of attention functioning (Sonuga-Barke and Castellanos, 2007; Sripada RK, in press). For example, Kelly and colleagues (2008) found that the degree of anti-correlation of these networks during the resting state predicted reaction time variability in a subsequent attention task. Of note, correlated activity between regions and networks is taken to represent

information-processing relationships (Bressler and Menon, 2010). Thus, somewhat speculatively, greater correlation between default and task-positive networks may represent increased interference by default network processes in task-positive operations. Overall, our finding that MPD produces reduces coupling of DMN and task positive ICNs thus adds to the evidence that dopamine enhances the competitive relationship between these networks, and raises the possibility that greater network segregation is involved in the mechanism by which MPD improves attention functioning.

This study has several limitations and raises issues that require further study. First, we performed resting state scanning roughly 60 minutes after administration of MPD, consistent with prior studies (Peterson et al., 2009; Rubia et al., 2009; Schweitzer et al., 2004). However, there is evidence that MPD produces peak effects roughly 90–120 minutes after administration (Muller et al., 2005; Wargin et al., 1983). Our placement of resting state scans prior to the peak window of methylphenidate effects may thus have resulted in diminished MPD effects and contributed additional variance, since drug-levels tend to be more stable after peak levels have been reached. Second, we used a grid-based parcellation method that places 1080 ROIs at regular intervals throughout the brain. This method uses partial sampling and averaging to down-sample the data, enhancing computational feasibility, but potentially losing useful discriminative information. Compared to other anatomical (e.g., Zeng et al., 2012) or functional (e.g., Dosenbach et al., 2010) parcellation schemes, our grid-based method does require placing substantially more ROIs, and thus may contribute many more irrelevant features to the classifier. It nonetheless has the advantage of minimizing a priori assumptions about the spatial distribution of methylphenidate effects. Future studies should directly compare the effectiveness of different ROI placement methods for connectomic fMRI pattern classification studies.

Our interpretation of decreases in functional connectivity in terms of network segregation requires clarification. We avoided use of global signal correction (‘global regression’) on our resting state time series because the method is capable of introducing artifactual negative correlations (Anderson et al., 2011a; Murphy et al., 2009). We used an alternative method for removing non-neuronal noise—WM/CSF correction with principal components analysis (see Methods for details)—which is unlikely to introduce these artifacts, though it may allow residual non-neuronal signals to persist (Fox et al., 2009). A main finding of this study is that MPD primarily produced decreases in connectivity, with MPD-attenuated edges exhibiting modest positive correlation during PBO, which became near zero, or weakly anti-correlated under MPD. We interpret this finding in terms of uncoupling of these regions due to MPD. However, another interpretation is possible if global noise remained in our resting state time series, despite our attempts at correction. If this is the case, it is likely we overestimated the baseline correlation at these edges, and these regions were in fact uncorrelated at baseline, and became modestly anti-correlated as a result of MPD [for a related discussion, see Anderson and colleagues (2011b)]. Thus our hypothesis of increased network segregation due to MPD might be interpreted either in terms of uncoupling or anti-correlations of networks depending on whether or not significant global noise remained in our data.

The methods used in this paper—connectomic imaging and multivariate pattern classification with paired SVM—have wide applicability in pharmaco-fMRI investigations. Psychoactive compounds are often predicted to affect distributed neurotransmitter systems (Cooper et al., 2002), producing widespread affects across the brain. In this context, standard seed-based methods coupled with mass univariate analysis present a dilemma for researchers. If just one or a handful of seeds are used, effects may be missed either due to erroneous a priori seed placement or failure to place seeds at all in certain regions. If too many seeds are used, the need to correct for multiple comparisons can dramatically reduce

power to detect effects. The multivariate connectomic methods used in the present study avoid this dilemma and provide researchers with a novel approach for investigating connectivity changes throughout the brain, while retaining sufficient power to detect drug-induced effects.

In summary, we used connectomic imaging coupled with multivariate pattern classification to investigate effects of MPD on resting state connectivity. We demonstrate that MPD produces a reliable multivariate neural signature encompassing multiple large-scale networks. Additionally, this study identifies promising new methods to probe distributed effects of drugs on the network structure of the brain.

Acknowledgments

C.S. Sripada's research was supported by the National Center for Advancing Translational Sciences of the National Institutes of Health under Award Number UL1TR000433, and NIH grant K23-AA-020297. C. Scott's research was supported by NIH grant P01CA087634.

References

Alexander GE, DeLong MR, Strick PL. Parallel organization of functionally segregated circuits linking basal ganglia and cortex. Annu Rev Neurosci. 1986; 9:357–381. [PubMed: 3085570]

Anderson JS, Druzgal TJ, Lopez-Larson M, Jeong EK, Desai K, Yurgelun-Todd D. Network anticorrelations, global regression, and phase-shifted soft tissue correction. Hum Brain Mapp. 2011a; 32:919–934. [PubMed: 20533557]

Anderson JS, Ferguson MA, Lopez-Larson M, Yurgelun-Todd D. Connectivity gradients between the default mode and attention control networks. Brain connectivity. 2011b; 1:147–157. [PubMed: 22076305]

Arnsten AFT, Li BM. Neurobiology of Executive Functions: Catecholamine Influences on Prefrontal Cortical Functions. Biological psychiatry. 2005; 57:1377–1384. [PubMed: 15950011]

Ashburner J. A fast diffeomorphic image registration algorithm. Neuroimage. 2007; 38:95–113. [PubMed: 17761438]

Beckmann CF, DeLuca M, Devlin JT, Smith SM. Investigations into resting-state connectivity using independent component analysis. Philosophical Transactions of the Royal Society B: Biological Sciences. 2005; 360:1001–1013.

Bishop CM. Pattern Recognition and Machine Learning, 1st ed. 2006. Corr. 2nd printing ed. Springer. 2007

Bressler SL, Menon V. Large-scale brain networks in cognition: emerging methods and principles. Trends Cogn Sci. 2010; 14:277–290. [PubMed: 20493761]

Brooks DJ. Functional imaging studies on dopamine and motor control. Journal of Neural Transmission. 2001; 108:1283–1298. [PubMed: 11768627]

Buhmann C, Glauche V, Sturenburg HJ, Oechsner M, Weiller C, Buchel C. Pharmacologically modulated fMRI--cortical responsiveness to levodopa in drug-naive hemiparkinsonian patients. Brain. 2003; 126:451–461. [PubMed: 12538411]

Clatworthy PL, Lewis SJG, Brichard L, Hong YT, Izquierdo D, Clark L, Cools R, Aigbirhio FI, Baron J-C, Fryer TD, Robbins TW. Dopamine Release in Dissociable Striatal Subregions Predicts the Different Effects of Oral Methylphenidate on Reversal Learning and Spatial Working Memory. The Journal of Neuroscience. 2009; 29:4690–4696. [PubMed: 19369539]

Cole DM, Oei NY, Soeter RP, Both S, van Gerven JM, Rombouts SA, Beckmann CF. Dopamine-Dependent Architecture of Cortico-Subcortical Network Connectivity. Cereb Cortex. 2012

Connolly MA, Liang KY. Conditional logistic regression models for correlated binary data. Biometrika. 1988; 75:501–506.

Cooper, JR.; Bloom, FE.; Roth, RH. The Biochemical Basis of Neuropharmacology. 8 ed. USA: Oxford University Press; 2002.

Corbetta M, Shulman GL. Control of goal-directed and stimulus-driven attention in the brain. Nature reviews. Neuroscience. 2002; 3:201–215. [PubMed: 11994752]

Cortes C, Vapnik V. Support-vector networks. Machine Learning. 1995; 20:273–297.

Cortese S, Kelly C, Chabernaud C, Proal E, Di Martino A, Milham MP, Castellanos FX. Toward Systems Neuroscience of ADHD: A Meta-Analysis of 55 fMRI Studies. Am J Psychiatry. 2012

Damoiseaux JS, Rombouts SA, Barkhof F, Scheltens P, Stam CJ, Smith SM, Beckmann CF. Consistent resting-state networks across healthy subjects. Proc Natl Acad Sci U S A. 2006; 103:13848–13853. [PubMed: 16945915]

Dosenbach NUF, Nardos B, Cohen AL, Fair DA, Power JD, Church JA, Nelson SM, Wig GS, Vogel AC, Lessov-Schlaggar CN, Barnes KA, Dubis JW, Feczko E, Coalson RS, Pruett JR, Barch DM, Petersen SE, Schlaggar BL. Prediction of Individual Brain Maturity Using fMRI. Science. 2010; 329:1358–1361. [PubMed: 20829489]

Fox MD, Snyder AZ, Vincent JL, Corbetta M, Van Essen DC, Raichle ME. The human brain is intrinsically organized into dynamic, anticorrelated functional networks. Proceedings of the National Academy of Sciences. 2005; 102:9673–9678.

Fox MD, Zhang D, Snyder AZ, Raichle ME. The global signal and observed anticorrelated resting state brain networks. Journal of neurophysiology. 2009; 101:3270–3283. [PubMed: 19339462]

Glover GH, Li TQ, Ress D. Image-based method for retrospective correction of physiological motion effects in fMRI: RETROICOR. Magnetic resonance in medicine: official journal of the Society of Magnetic Resonance in Medicine / Society of Magnetic Resonance in Medicine. 2000; 44:162–167. [PubMed: 10893535]

Greicius MD, Krasnow B, Reiss AL, Menon V. Functional connectivity in the resting brain: a network analysis of the default mode hypothesis. Proc Natl Acad Sci U S A. 2003; 100:253–258. [PubMed: 12506194]

Guyon I, Elisseeff A. An introduction to variable and feature selection. J. Mach. Learn. Res. 2003; 3:1157–1182.

Hampshire A, Owen AM. Fractionating Attentional Control Using Event-Related fMRI. Cerebral Cortex. 2006; 16:1679–1689. [PubMed: 16436686]

Hannestad J, Gallezot JD, Planeta-Wilson B, Lin SF, Williams WA, van Dyck CH, Malison RT, Carson RE, Ding YS. Clinically relevant doses of methylphenidate significantly occupy norepinephrine transporters in humans in vivo. Biological Psychiatry. 2010; 68:854–860. [PubMed: 20691429]

Haslinger B, Erhard P, Kampfe N, Boecker H, Rummeny E, Schwaiger M, Conrad B, Ceballos-Baumann AO. Event-related functional magnetic resonance imaging in Parkinson's disease before and after levodopa. Brain. 2001; 124:558–570. [PubMed: 11222456]

Heinzle J, Wenzel MA, Haynes JD. Visuomotor functional network topology predicts upcoming tasks. J Neurosci. 2012; 32:9960–9968. [PubMed: 22815510]

Hoshi E, Tremblay L, Feger J, Carras PL, Strick PL. The cerebellum communicates with the basal ganglia. Nat Neurosci. 2005; 8:1491–1493. [PubMed: 16205719]

Kelly AM, Uddin LQ, Biswal BB, Castellanos FX, Milham MP. Competition between functional brain networks mediates behavioral variability. Neuroimage. 2008; 39:527–537. [PubMed: 17919929]

Kelly C, de Zubicaray G, Di Martino A, Copland DA, Reiss PT, Klein DF, Castellanos FX, Milham MP, McMahon K. L-dopa modulates functional connectivity in striatal cognitive and motor networks: a double-blind placebo-controlled study. The Journal of neuroscience: the official journal of the Society for Neuroscience. 2009; 29:7364–7378. [PubMed: 19494158]

Laird AR, Fox PM, Eickhoff SB, Turner JA, Ray KL, McKay DR, Glahn DC, Beckmann CF, Smith SM, Fox PT. Behavioral interpretations of intrinsic connectivity networks. J Cogn Neurosci. 2011; 23:4022–4037. [PubMed: 21671731]

Li SJ, Biswal B, Li Z, Risinger R, Rainey C, Cho JK, Salmeron BJ, Stein EA. Cocaine administration decreases functional connectivity in human primary visual and motor cortex as detected by functional MRI. Magn Reson Med. 2000; 43:45–51. [PubMed: 10642730]

Liddle EB, Hollis C, Batty MJ, Groom MJ, Totman JJ, Liotti M, Scerif G, Liddle PF. Task-related default mode network modulation and inhibitory control in ADHD: effects of motivation and

methylphenidate. Journal of Child Psychology and Psychiatry. 2011; 52:761–771. [PubMed: 21073458]

Marquand AF, Simoni SD, O'Daly OG, Williams SCR, Mourao-Miranda J, Mehta MA. Pattern Classification of Working Memory Networks Reveals Differential Effects of Methylphenidate, Atomoxetine, and Placebo in Healthy Volunteers. Neuropsychopharmacology. 2011; 36:1237–1247. [PubMed: 21346736]

McAvoy M, Larson-Prior L, Ludwikow M, Zhang D, Snyder AZ, Gusnard DL, Raichle ME, d'Avossa G. Dissociated mean and functional connectivity BOLD signals in visual cortex during eyes closed and fixation. Journal of neurophysiology. 2012

McClure SM, Daw ND, Montague PR. A computational substrate for incentive salience. Trends in neurosciences. 2003; 26:423–428. [PubMed: 12900173]

McKiernan KA, Kaufman JN, Kucera-Thompson J, Binder JR. A parametric manipulation of factors affecting task-induced deactivation in functional neuroimaging. J Cogn Neurosci. 2003; 15:394–408. [PubMed: 12729491]

Mehta MA, Goodyer IM, Sahakian BJ. Methylphenidate improves working memory and set-shifting in AD/HD: relationships to baseline memory capacity. Journal of Child Psychology and Psychiatry, and Allied Disciplines. 2004; 45:293–305.

Menon V. Large-scale brain networks and psychopathology: a unifying triple network model. Trends Cogn Sci. 2011; 15:483–506. [PubMed: 21908230]

Menon V, Uddin LQ. Saliency, switching, attention and control: a network model of insula function. Brain Struct Funct. 2010; 214:655–667. [PubMed: 20512370]

Montgomery AJ, Asselin MC, Farde L, Grasby PM. Measurement of methylphenidate-induced change in extrastriatal dopamine concentration using [11C]FLB 457 PET. Journal of Cerebral Blood Flow and Metabolism: Official Journal of the International Society of Cerebral Blood Flow and Metabolism. 2007; 27:369–377. [PubMed: 16685253]

Muller U, Suckling J, Zelaya F, Honey G, Faessel H, Williams SC, Routledge C, Brown J, Robbins TW, Bullmore ET. Plasma level- dependent effects of methylphenidate on task-related functional magnetic resonance imaging signal changes. Psychopharmacology (Berl). 2005; 180:624–633. [PubMed: 15830222]

Murphy K, Birn RM, Handwerker DA, Jones TB, Bandettini PA. The impact of global signal regression on resting state correlations: are anti-correlated networks introduced? Neuroimage. 2009; 44:893–905. [PubMed: 18976716]

Mwangi B, Ebmeier KP, Matthews K, Steele JD. Multi-centre diagnostic classification of individual structural neuroimaging scans from patients with major depressive disorder. Brain: a journal of neurology. 2012; 135:1508–1521. [PubMed: 22544901]

Nagano-Saito A, Leyton M, Monchi O, Goldberg YK, He Y, Dagher A. Dopamine depletion impairs frontostriatal functional connectivity during a set-shifting task. The Journal of neuroscience: the official journal of the Society for Neuroscience. 2008; 28:3697–3706. [PubMed: 18385328]

Nauhaus I, Busse L, Carandini M, Ringach DL. Stimulus contrast modulates functional connectivity in visual cortex. Nature neuroscience. 2009; 12:70–76.

Nieoullon A. Dopamine and the regulation of cognition and attention. Progress in Neurobiology. 2002; 67:53–83. [PubMed: 12126656]

Ochsner KN, Gross JJ. The cognitive control of emotion. Trends Cogn Sci. 2005; 9:242–249. [PubMed: 15866151]

Peterson BS, Potenza MN, Wang Z, Zhu H, Martin A, Marsh R, Plessen KJ, Yu S. An FMRI study of the effects of psychostimulants on defaultmode processing during Stroop task performance in youths with ADHD. Am J Psychiatry. 2009; 166:1286–1294. [PubMed: 19755575]

Posner MI, Rothbart MK. Research on attention networks as a model for the integration of psychological science. Annual review of psychology. 2007; 58:1–23.

Raichle ME, MacLeod AM, Snyder AZ, Powers WJ, Gusnard DA, Shulman GL. A default mode of brain function. Proc Natl Acad Sci U S A. 2001; 98:676–682. [PubMed: 11209064]

Ramos BP, Arnsten AFT. Adrenergic pharmacology and cognition: Focus on the prefrontal cortex. Pharmacology & Therapeutics. 2007; 113:523–536. [PubMed: 17303246]

Ricciardi E, Handjaras G, Bernardi G, Pietrini P, Furey ML. Cholinergic enhancement reduces functional connectivity and BOLD variability in visual extrastriate cortex during selective attention. Neuropharmacology. 2012

Robbins TW. Chemistry of the mind: neurochemical modulation of prefrontal cortical function. The Journal of comparative neurology. 2005; 493:140–146. [PubMed: 16254988]

Rubia K, Halari R, Cubillo A, Mohammad AM, Brammer M, Taylor E. Methylphenidate normalises activation and functional connectivity deficits in attention and motivation networks in medication-naive children with ADHD during a rewarded continuous performance task. Neuropharmacology. 2009; 57:640–652. [PubMed: 19715709]

Schiffer WK, Volkow ND, Fowler JS, Alexoff DL, Logan J, Dewey SL. Therapeutic doses of amphetamine or methylphenidate differentially increase synaptic and extracellular dopamine. Synapse (New York, N.Y.). 2006; 59:243–251.

Schlosser RG, Nenadic I, Wagner G, Zysset S, Koch K, Sauer H. Dopaminergic modulation of brain systems subserving decision making under uncertainty: a study with fMRI and methylphenidate challenge. Synapse. 2009a; 63:429–442. [PubMed: 19184997]

Schlosser, RGm; Nenadic, I.; Wagner, G.; Zysset, S.; Koch, K.; Sauer, H. Dopaminergic modulation of brain systems subserving decision making under uncertainty: A study with fMRI and methylphenidate challenge, Dopaminergic modulation of brain systems subserving decision making under uncertainty: A study with fMRI and methylphenidate challenge. Synapse, Synapse. 2009b; 63 63, 429, 429–442, 442–429, 429–442, 442.

Scholkopf B, Platt JC, Shawe-Taylor J, Smola AJ, Williamson RC. Estimating the Support of a High-Dimensional Distribution. Neural Computation. 2001; 13:1443–1471. [PubMed: 11440593]

Schweitzer JB, Lee DO, Hanford RB, Zink CF, Ely TD, Tagamets MA, Hoffman JM, Grafton ST, Kilts CD. Effect of methylphenidate on executive functioning in adults with attention-deficit/hyperactivity disorder: normalization of behavior but not related brain activity. Biol Psychiatry. 2004; 56:597–606. [PubMed: 15476690]

Scott, C. Communications and Signal Processing Laboratory. Ann Arbor, MI: University of Michigan; 2012. The equivalence between the one-class and paired support vector machines for nonseparable data. Tech. Rep. CSPL-412. http://www.eecs.umich.edu/techreports/systems/cspl/cspl-412.pdf

Sonuga-Barke EJS, Castellanos FX. Spontaneous attentional fluctuations in impaired states and pathological conditions: A neurobiological hypothesis. Neuroscience & Biobehavioral Reviews. 2007; 31:977–986. [PubMed: 17445893]

Sripada RK, K A, Welsh RC, Garfinkel SN, Wang X, Sripada CS, Liberzon I. Disrupted Equilibrium between Salience Network and Default Mode Network in Posttraumatic Stress Disorder. Psychosomatic Medicine. in press.

Swanson J, Baler RD, Volkow ND. Understanding the effects of stimulant medications on cognition in individuals with attention-deficit hyperactivity disorder: a decade of progress. Neuropsychopharmacology: Official Publication of the American College of Neuropsychopharmacology. 2011; 36:207–226. [PubMed: 20881946]

Tomasi D, Volkow ND, Wang GJ, Wang R, Telang F, Caparelli EC, Wong C, Jayne M, Fowler JS. Methylphenidate enhances brain activation and deactivation responses to visual attention and working memory tasks in healthy controls. Neuroimage. 2011; 54:3101–3110. [PubMed: 21029780]

Tost H, Braus DF, Hakimi S, Ruf M, Vollmert C, Hohn F, Meyer-Lindenberg A. Acute D2 receptor blockade induces rapid, reversible remodeling in human cortical-striatal circuits. Nature neuroscience. 2010; 13:920–922.

Tzourio-Mazoyer N, Landeau B, Papathanassiou D, Crivello F, Etard O, Delcroix N, Mazoyer B, Joliot M. Automated anatomical labeling of activations in SPM using a macroscopic anatomical parcellation of the MNI MRI single-subject brain. Neuroimage. 2002; 15:273–289. [PubMed: 11771995]

Volkow ND, Fowler JS, Wang G, Ding Y, Gatley SJ. Mechanism of action of methylphenidate: insights from PET imaging studies. Journal of Attention Disorders. 2002; 1(6 Suppl) S31-43-S31-43.

Volkow ND, Wang GJ, Fowler JS, Gatley SJ, Logan J, Ding YS, Hitzemann R, Pappas N. Dopamine transporter occupancies in the human brain induced by therapeutic doses of oral methylphenidate. The American Journal of Psychiatry. 1998; 155:1325–1331. [PubMed: 9766762]

Wargin W, Patrick K, Kilts C, Gualtieri CT, Ellington K, Mueller RA, Kraemer G, Breese GR. Pharmacokinetics of methylphenidate in man, rat and monkey. The Journal of pharmacology and experimental therapeutics. 1983; 226:382–386. [PubMed: 6410043]

Weissman DH, Roberts KC, Visscher KM, Woldorff MG. The neural bases of momentary lapses in attention. Nat Neurosci. 2006; 9:971–978. [PubMed: 16767087]

Yeo BT, Krienen FM, Sepulcre J, Sabuncu MR, Lashkari D, Hollinshead M, Roffman JL, Smoller JW, Zollei L, Polimeni JR, Fischl B, Liu H, Buckner RL. The organization of the human cerebral cortex estimated by intrinsic functional connectivity. J Neurophysiol. 2011; 106:1125–1165. [PubMed: 21653723]

Zeng L-L, Shen H, Liu L, Wang L, Li B, Fang P, Zhou Z, Li Y, Hu D. Identifying major depression using whole-brain functional connectivity: a multivariate pattern analysis. Brain: a journal of neurology. 2012; 135:1498–1507. [PubMed: 22418737]

Highlights

- We examine effects of methylphenidate (MPD) on resting state functional connectivity
- 32 subjects, within-subject, double-blind, placebo-controlled, randomized, counterbalanced, cross-over design
- Resting state connectomes analyzed with paired support vector machine classifiers
- MPD impacted motor processing networks, and reduced coupling within visual network
- MPD enhanced segregation of default network and task positive networks

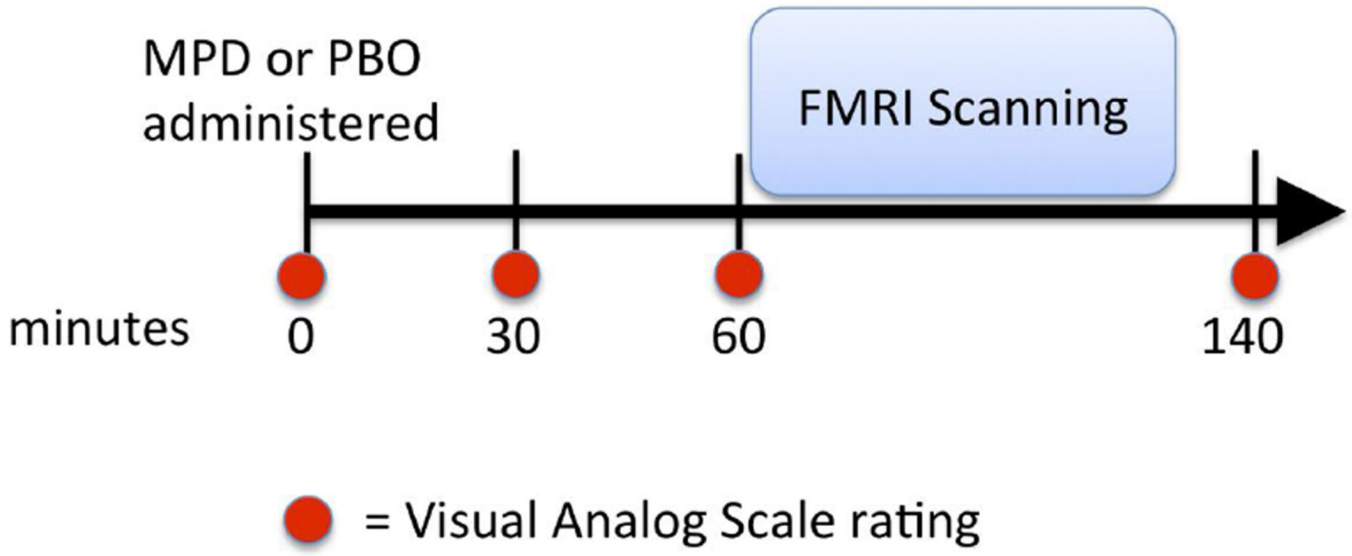

Figure 1.
Sequence of events during pharmaco-fMRI experiment.

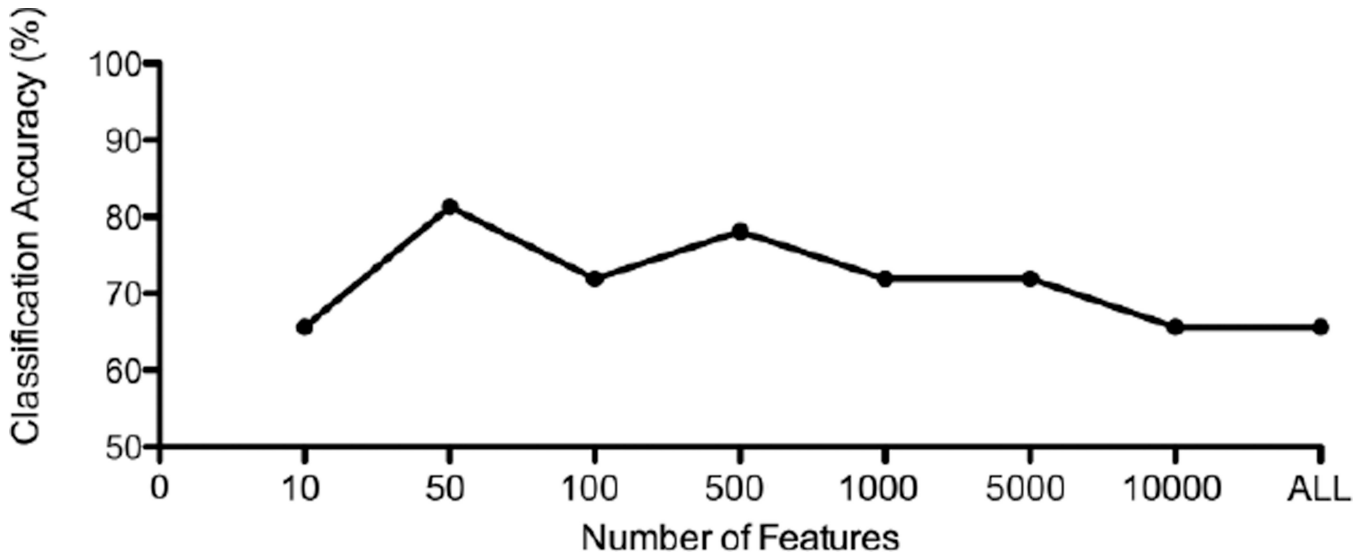

Figure 2.
Classification Accuracy versus Feature Space Size. ALL = all the features.

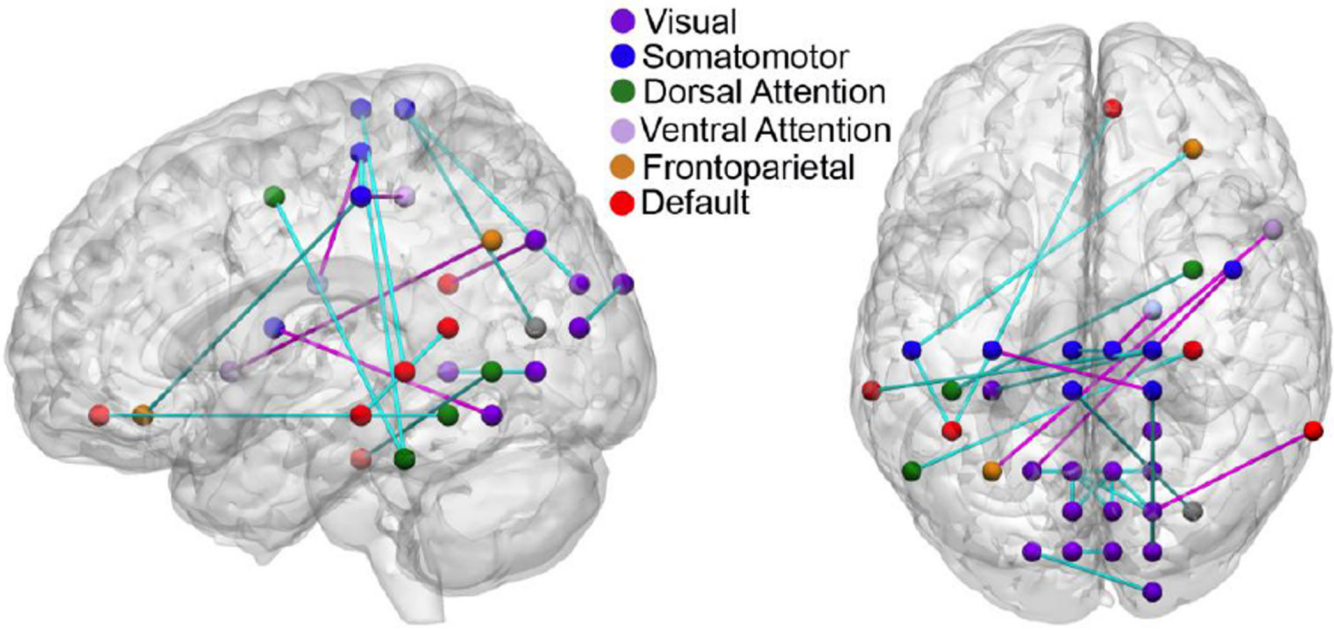

Figure 3.
50 feature classifier: Consensus connectome. A support vector machine classifier was trained to distinguish methylphenidate (MPD) and placebo (PBO) resting state connectomes. Major networks within the consensus connectome, which served as the basis of classification, are shown overlaid on a canonical brain. Methylphenidate effects were concentrated in the visual, somatomotor, and default networks. Network affiliations of nodes were assigned on an a priori basis according to the network parcellation map of Yeo and colleagues (2011).

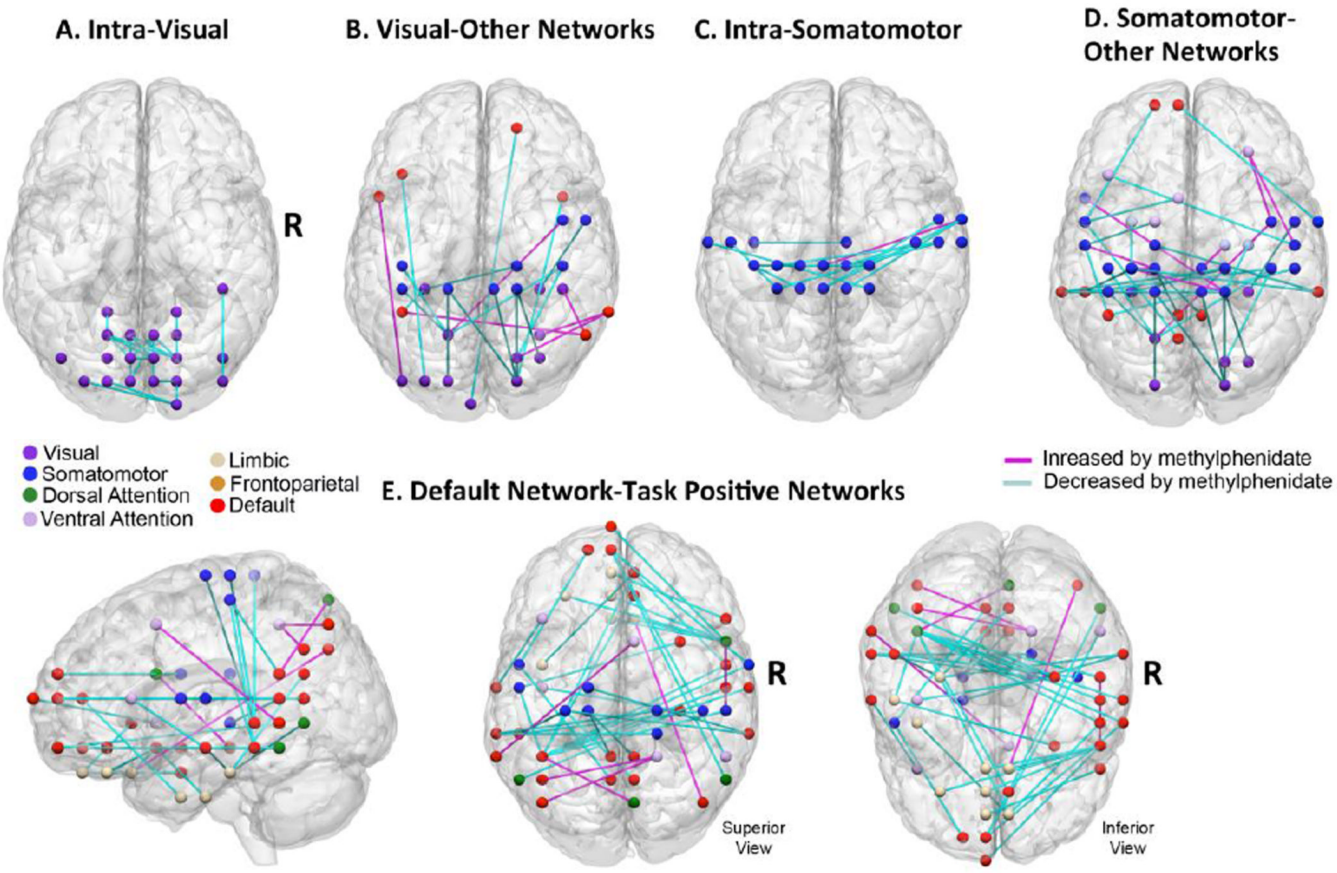

Figure 4.

500 feature classifier: Consensus connectome. Methylphenidate reduced connectivity within visual network and somatomotor networks (top panels). In addition, methylphenidate reduced default network connectivity with multiple task positive networks (bottom panel). Network affiliations of nodes were assigned on an a priori basis according to the network parcellation map of Yeo and colleagues (2011).

Table 1

50 feature classifier: Descriptive summary of the consensus connectome. The edges of the consensus connectome were cross-tabulated with respect to major intrinsic connectivity networks as well as striatum. The number of edges that are associated with each pair of networks is indicated by the main entries, and number of edges that *decreased* in strength is indicated within parentheses. 'Total' refers to the total number of edges that involve the respective network (i.e., at least one node of the edge is in the network).

	Visual	**Somato-motor**	**Dorsal Attention**	**Ventral Attention**	**Limbic**	**Fronto-parietal**	**Default**	**Straitum**	**All Other Areas**
Visual	10 (10)	3 (2)	0 (0)	0 (0)	0 (0)	0 (0)	1 (0)	0 (0)	0 (0)
Somato- motor		1 (1)	0 (0)	1 (0)	0 (0)	1 (1)	1 (1)	1 (1)	1 (1)
Dorsal attention			0 (0)	0 (0)	0 (0)	0 (0)	2 (2)	0 (0)	0 (0)
Ventral attention				0 (0)	0 (0)	1 (0)	0 (0)	0 (0)	0 (0)
Limbic					0 (0)	0 (0)	0 (0)	0 (0)	0 (0)
Fronto-parietal						0 (0)	0 (0)	0 (0)	0 (0)
Default							1 (1)	0 (0)	1 (1)
Striatum								0 (0)	0 (0)
All Other Areas									0 (0)
Total	14	9	3	2	0	2	6	8	2

Table 2

500 feature classifier: Descriptive summary of the consensus connectome. The cross-tabulation shows the edges of the consensus connectome in terms of their affiliation with major intrinsic connectivity networks as well as striatum. The number of edges that are associated with each pair of networks is indicated by the main entries, and number of edges that *decreased* in strength is indicated within parentheses. 'Total' refers to the total number of edges that involve the respective network (i.e., at least one node of the edge is in the network).

	Visual	**Somato-motor**	**Dorsal Attention**	**Ventral Attention**	**Limbic**	**Fronto-parietal**	**Default**	**Straitum**	**All Other Areas**
Visual	27 (27)	12 (11)	4 (2)	3 (2)	3 (2)	4 (0)	9 (4)	2 (2)	5 (5)
Somato- motor		28 (27)	2 (1)	7 (3)	3 (2)	4 (2)	13 (13)	5 (2)	5 (5)
Dorsal attention			3 (3)	3 (1)	3 (1)	1 (0)	9 (7)	1 (0)	2 (2)
Ventral attention				1 (1)	2 (2)	5 (1)	6 (3)	2 (1)	5 (1)
Limbic					0 (0)	1 (0)	10 (9)	1 (1)	1 (1)
Fronto-parietal						0 (0)	2 (1)	4 (1)	2 (0)
Default							8 (8)	5 (2)	18 (13)
Striatum								0 (0)	5 (1)
All Other Areas									4 (2)
Total	69	79	28	34	24	23	80	25	47

Neuroimage. Author manuscript; available in PMC 2014 November 01.